Numerical Investigation of Internal Wave-Vortex Interactions

Tyler D. Blackhurst and J.C. Vanderhoff
Department of Mechanical Engineering
Brigham Young University, Provo, UT

Abstract

Internal gravity waves are inherent in the atmosphere due to its stable stratification. They may be generated in many ways, including by flow over topography, convective storms, or turbulent mixing. As they propagate through the atmosphere and ocean, internal waves of various scales (tens of meters to tens of kilometers) interact with various phenomena found throughout geophysical fluid flows. The interaction of small-scale internal waves with a vortex dipole is of particular interest because of their frequency in nature due to the rotation of the earth resulting in constant vortex generation. The speed and direction with which internal waves approach a vortex dipole can significantly affect the wave-vortex interaction, determining if the energy of the internal waves will be absorbed, refracted, or unaffected by the dipole. Variations of this interaction are investigated through three-dimensional linear and nonlinear numerical simulations. The linear theory is ideal due to the speed of calculations: tens of thousands of waves can be tested in a few hours using a standard PC. Physical dynamics of possible interactions are quantified through the calculations of basic wave parameters and amplitudes and the results agree qualitatively with experimentation. Fully nonlinear simulations and experimental results are used to validate the linear theory.

Introduction

A stably-stratified fluid is one in which the density increases continuously with depth, such as the ocean or the atmosphere. Perturbations of a stably-stratified fluid, such as tidal flow over topography, move fluid particles of one depth and neutrally-buoyant state to a depth in which they are surrounded by fluid particles of a different density. The surrounding fluid particles push the displaced particles back in the direction of their neutrally-buoyant state. When there is enough momentum to displace the fluid particles in the other direction, oscillations occur until the fluid particles reach a stable location with respect to their density. The oscillations are defined by the Brunt-Väisälä frequency, the natural frequency of the fluid, which involves the change in density over height within the fluid. Oscillations less than this frequency create internal waves which play an integral role in oceanic and atmospheric dynamics.

Since early last century scientists and researchers have observed and studied internal wave propagation and evolution in stratified fluids, especially in the ocean and atmosphere. Today researchers can numerically simulate internal wave propagation and wave interactions with other fluid phenomena, studying them from every point in space and time, and compare the results with what is known from observation and experimentation. However, reconciling theoretical predictions with experimental data is sometimes problematic since, during wave propagation and interactions, the transport of energy may be at such small scales that observations lack sufficient resolution and the onset of turbulence invalidates two-dimensional linear theories. With three-dimensional-simulation capabilities, we can more completely study scenarios involving internal waves in the ocean and atmosphere and apply more accurate theories and approximations.

Internal waves interact with a myriad of flow phenomena, including other internal waves of similar and different scales. Javam, Imberger and Armfield (2000) numerically researched interactions of internal waves of similar scales and found these interactions were nonlinear and involved wave breaking. Broutman and Young (1986) used ray theory (to be described later) to numerically track the changes of small-scale internal waves (on the order of tens of meters) interacting with a large-scale internal wave background (on the order of kilometers and greater). They confirmed theoretical predictions for conditions of internal waves prior to and following the interactions. Winters and D'Asaro (1989) used a two-dimensional model to numerically simulate the propagation of internal waves into a slowly-varying mean shear background. Nonlinearity and three-dimensionality overcome the simulated waves when the internal waves become unstable and turbulence begins, breaking down the internal waves. Later, three-dimensional considerations were discussed in Winter and D'Asaro (1994). Convective instabilities yielded counter-rotating vortices, the effects of which were magnified by wave shear. The combination of convection and shear in these interactions obligate three-dimensional analysis. This obligation is a representative result of all the studies cited thus far and is essential to the continuing discussion.

Vortices are a common occurrence in large, geophysical flows as a result of shear and turbulence in a rotating fluid. Moulin and Flór (2006) numerically demonstrated a three-dimensional interaction between a large-scale internal wave and a Rankine-type vortex. By varying the initial locations of the internal waves, the authors demonstrated that each wave-vortex interaction resulted in a different scenario with different effects on the internal waves. In some cases, the waves reflected; in others, they were absorbed into the rotating flow; still other combinations produced breaking waves. Despite the wealth of information gained from these simulations, questions remain about what happens to the energy of internal waves during the onset of turbulence and other three-dimensional characteristics during wave-vortex interactions. While we know the waves may break, it is unclear what mechanisms are responsible for their evolution to breaking and how and why turbulence begins.

Godoy-Diana, Chomaz and Donnadieu (2006) discussed the experimental interaction of internal waves with a Lamb-Chaplygin pancake vortex dipole. A vortex dipole involves two side-by-side, counter-rotating vortices; the Lamb-Chaplygin vortex dipole is an exact solution of the Euler equations (Billant, Brancher and Chomaz (1999)). Two scenarios of wave-vortex interactions were conducted: one in which the internal wave's horizontal wave number propagated with the flow and one in which it propagated against the flow. The former scenario showed the wave beam bending to the horizontal and possibly being absorbed by the vortex. The latter scenario resulted in the beam of internal waves steepening to the vertical and possibly reflecting. The results of this experiment suggest three-dimensional effects are essential in internal wave propagation. A numerical analysis of this experiment illuminates the three-dimensional mechanisms of these effects, showing what happens to the internal wave properties and energy during internal wave interactions.

This paper details the work that has been done and discusses work to still be done to numerically model a set of small-scale internal waves interacting in three dimensions with a vortex dipole of constant propagation. The Methods section discusses the experimental setup of Godoy-Diana *et. al.* (2006) and the corresponding numerical setup for the current study, and presents the mathematical theory involved. The next section presents the results of the interaction simulations, including comparisons to the experiment of Godoy-Diana *et. al.* (2006). The final section discusses the practical impact of the results of the study, further research to be done on this project, and ideas for future research.

Methods

The experimental internal wave-vortex interaction of Godoy-Diana *et. al.* (2006) was completed in a salt-stratified water tank as shown in Figure 1. The dipole is created and then approaches a screen which allows only a thin slice of the dipole to pass to the area of interaction. The internal-wave beams are generated by oscillating a cylinder at a frequency less than the natural buoyancy frequency of the fluid, which was maintained constant. Figure 2 shows a close-up view of two scenarios of interactions: co-propagating, in which the waves propagate in the same direction as the vortex direction of propagation; and counter-propagating, in which the waves propagate opposite to the vortex direction of propagation. The general anticipated outcome of the experiment can be seen as the co-propagating representation of the wave beam is absorbed into the flow of the vortex, and the counter-propagating representation of the wave beam is reflected away from the vortex.

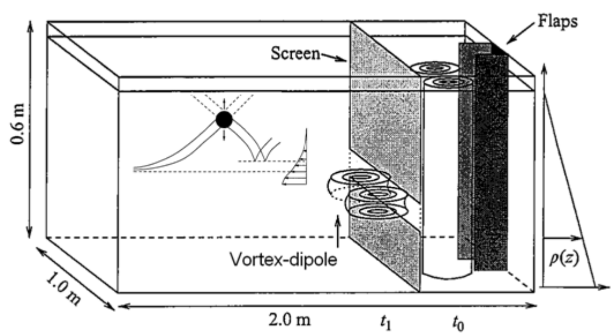

Figure 1: Saltwater stratified water experimental tank (Godoy-Diana, *et. al.* (2006)). The dipole is created by flaps at one end of the tank and approaches a screen which allows a slice of the dipole to pass into the interaction area with the cylinder generating the internal waves.

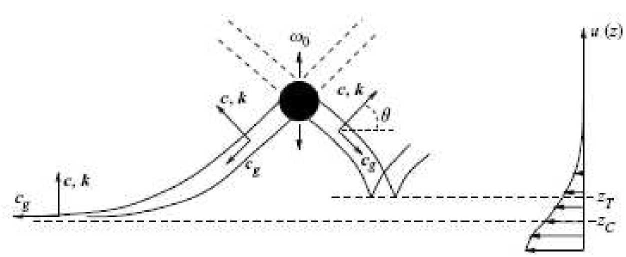

Figure 2: Close-up view of oscillating cylinder generating internal waves relative to the vortex velocity profile (Godoy-Diana, *et. al.* (2006)). The co-propagating case shows the internal waves being absorbed by the vortex. The counter-propagating case shows the internal waves reflecting away from the vortex.

The numerical code for the current study was written in Matlab. It has been modified from previous two-dimensional code and developed for three-dimensional simulations. It has been organized to consider individually the same two scenarios of interaction carried out in its experimental counterpart. At the code's core, ray theory governs the numerical simulation. Ray theory, often called ray tracing, traces the directions (rays) of small-amplitude internal wave propagation before, during, and after the wave-vortex interaction. Ray theory is linear, even in three dimensions, so the basic propagation of the waves can be simply modeled. In addition, calculations are made to analyze wave amplitudes which may result in wave breaking. Ray theory efficiently tracks internal wave propagation and the results easily compare to those of the experiment. Ray theory is also quick in its application, providing a method of research much faster and less expensive than experimentation and observation.

Ray theory is a method of solving the Navier-Stokes equations, the governing equations of fluid flow. To simplify the Navier-Stokes equations for this case, the propagation of the vortex is assumed slowly varying while the only side-effects of the interaction are changes to the characteristics and propagation of the small-scale internal waves. This is the linear, inviscid Wentzel-Kramer-Brillouin (WKB) approximation. It allows the dispersion relation to be valid locally. While it is not representative of all wave-vortex interactions, this assumption is realistic when waves are interacting with large-scale geophysical flows and is the foundation of ray theory. Another simplification is the Boussinesq approximation, which states that changes in density are negligible except in terms where the acceleration due to gravity is a multiplier. The solution to the Navier-Stokes equations is then in a form of the wave equation.

To verify that the correct equations are being solved for this simulation, the equations have been rederived and their accuracy of implementation in the code confirmed. The full ray theory equations for a mean velocity field $\boldsymbol{V}=(v_1,v_2,v_3)$ through which the internal waves propagate with frequency relative to the background are now presented.

The Doppler relation defines the relation between the frequencies of the background Ω and the frequency of the internal wave ω_r,

$$\omega_r = \Omega - v_j k_j \tag{1}$$

where v_j is the component of the background velocity and k_j is the component of the small-scale wavenumber vector $\boldsymbol{k}=(k_1,k_2,k_3)$ in the same direction. The dispersion relation defines ω_r as a function of wavenumber, the buoyancy frequency N, and the Coriolis force (which is insignificant for the simulations at hand),

$$\omega_r^2 = \frac{N^2(k_1^2+k_2^2)+f^2m^2}{k_1^2+k_2^2+k_3^2} \tag{2}$$

The velocities of the internal waves are defined by the sum of the background velocity and the group velocity of the internal waves,

$$\frac{dx_i}{dt} = v_i + \frac{\partial \omega}{\partial k_i} \tag{3}$$

for which $\boldsymbol{x}=(x_1,x_2,x_3)$ defines the space of the domain and where

$$\begin{aligned}\frac{\partial \omega_r}{\partial k_1} &= -k_1(k_1^2+k_2^2+k_3^2)^{-3/2}\left[N^2(k_1^2+k_2^2)+f^2k_3^2\right]^{1/2} \\ &+ N^2k_1(k_1^2+k_2^2+k_3^2)^{-1/2}\left[N^2(k_1^2+k_2^2)+f^2k_3^2\right]^{1/2}\end{aligned} \tag{3}$$

$$\begin{aligned}\frac{\partial \omega_r}{\partial k_2} &= -k_2(k_1^2+k_2^2+k_3^2)^{-3/2}\left[N^2(k_1^2+k_2^2)+f^2k_3^2\right]^{1/2} \\ &+ N^2k_2(k_1^2+k_2^2+k_3^2)^{-1/2}\left[N^2(k_1^2+k_2^2)+f^2k_3^2\right]^{1/2}\end{aligned} \tag{4}$$

and

$$\begin{aligned}\frac{\partial \omega_r}{\partial k_3} &= -k_3(k_1^2+k_2^2+k_3^2)^{-3/2}\left[N^2(k_1^2+k_2^2)+f^2k_3^2\right]^{1/2} \\ &+ N^2k_3(k_1^2+k_2^2+k_3^2)^{-1/2}\left[N^2(k_1^2+k_2^2)+f^2k_3^2\right]^{1/2}\end{aligned} \tag{5}$$

The law governing refraction is given by

$$\frac{dk_i}{dt} = -k_j\frac{\partial v_j}{\partial x_i} - \frac{\partial \omega_r}{\partial x_i} \tag{6}$$

To define the change of the relative frequency with respect to time,

$$\frac{d\omega_r}{dt} = \frac{\partial \omega_r}{\partial k_i}\frac{dk_i}{dt} + \frac{\partial \omega_r}{\partial x_i}\frac{dx_i}{dt} \tag{7}$$

For this simulation, the partial derivative of ω_r with respect to space is zero because $\boldsymbol{k}$, N, nor f in the dispersion relation are functions of space. Thus the last two equations reduce to only their first terms on the right hand side.

Results

To validate the results of the numerical simulations, the conditions of the experiments of Godoy-Diana, *et. al.* (2006) were input to the code. Figure 3 shows the initial representation of the lines of wave propagation for the co-propagating wave-vortex interaction in a three-dimensional domain.

pass through the vortex at angles different than their initial angle. This is due to changes in their properties, such as wave number.

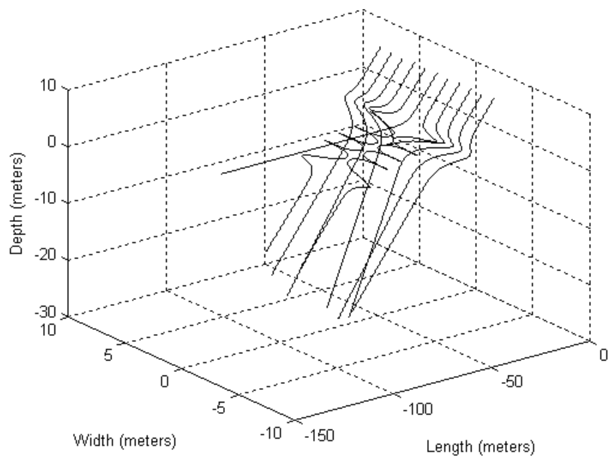

Figure 3: Initial results of the numerical co-propagating scenario. The lines are the rays traced by ray theory and represent internal waves at various initial locations. They all begin at the same position along the length and the depth in the domain, but at different positions along the width.

The lines are the rays tracing various internal waves. The waves begin at the same position along the length and along the depth of the domain, but at different positions along the width. They also begin with the same wave numbers. By following the rays, it is clear that the interaction is being, in general, appropriately represented. That is, the lines/rays representing the movement of the internal waves over time follow the patterns expected in an interaction with a vortex dipole: the center ray moves quickly along the length of the domain, never wavering; one of the inner rays on either side of the center ray are caught for a time in the vortex; outer rays are affected by the vortex velocity field, but escape through its underside.

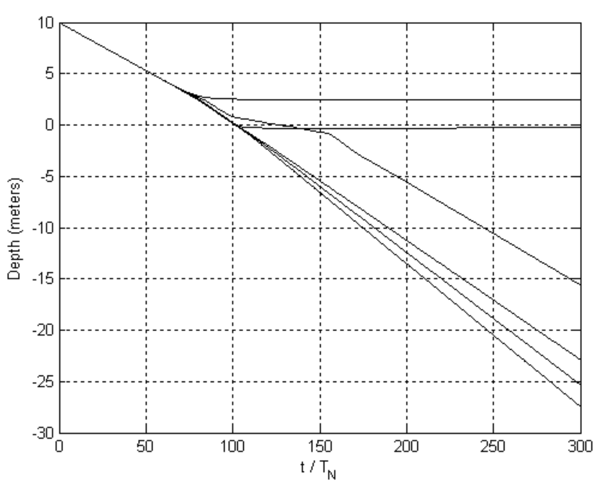

Figure 4: View of numerical solution showing how rays change along the depth with respect to a nondimensional time t/T_N, where T_N is the buoyancy period of the fluid. The top ray is the center ray of Figure 3, and is entirely absorbed by the vortex. Other rays are also shown being absorbed. Still other rays are affected by the interaction but pass through the vortex at angles different than their initial angle. This is due to changes in their properties, such as wave number.

Figure 4 shows a view of how the rays change along the depth of the tank with respect to a nondimensional time t / T_N, where T_N is the buoyancy period of the fluid. In this view, it is seen how the rays change their angles of propagation, inferring also changes to their properties. Figure 5 shows a similar result from the experimental counterpart, and can be compared to the center ray of Figures 3 and 4. Figure 5a shows the beams of internal waves before interaction with the dipole. Figure 5b shows one of the beams bending to the velocity profile of the dipole. Figures 5c and 5d show the beams being more absorbed into the vortex. Figures 4 and 5 in comparison demonstrate qualitatively that the code is performing as expected. Some rays are being absorbed, based on their initial location, while others are passing through the vortex dipole with new properties. These rays passing through show other interactions not considered in the experimental counterpart to this numerical study. There are many possible interactions still to be discovered.

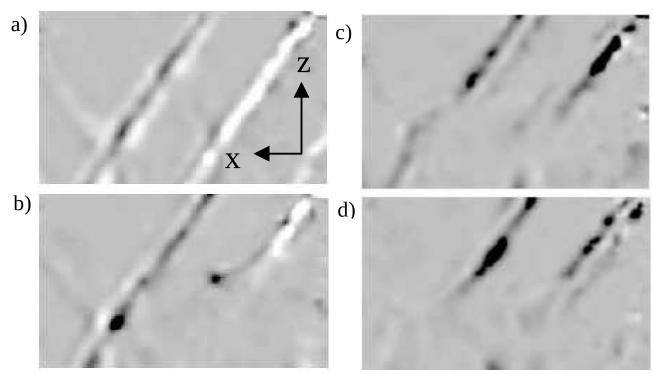

Figure 5: View of experimental results from Godoy-Diana, *et. al.* (2006) for the co-propagating scenario showing the wave beams changing along the depth with respect to the length of the tank. 5a shows the internal wave beams prior to the interaction, 5b shows one wave beam being absorbed by the interaction. 5c and d show the evolution of the interaction as the vortex absorbs the wave beams.

It is the change in properties that is particularly interesting. Depending on the changes of wave numbers and amplitude, the waves may in some cases be approaching breaking and turbulence. While ray tracing cannot follow or predict these nonlinear characteristics due to internal wave interactions, it can help predict their evolution to breaking and turbulence. Then, as the waves begin to overturn, a point of breaking can be determined.

Discussion

Despite the expected quantitative demonstration of the correct flow pattern of the interaction, the initial results do not yield the solutions of Godoy-Diana *et. al.* (2006), and full analysis of the interaction is not yet possible. Upon further investigation, several errors have become known.

First, it was discovered that time dependence of the second wave number k_2 had been neglected. As a result, this property of the internal waves was maintained constant rather than changing according to (6). Without the necessary changes to the wavenumber vector, the rays after the interaction do not accurately predict the actual physical state of the individual internal waves.

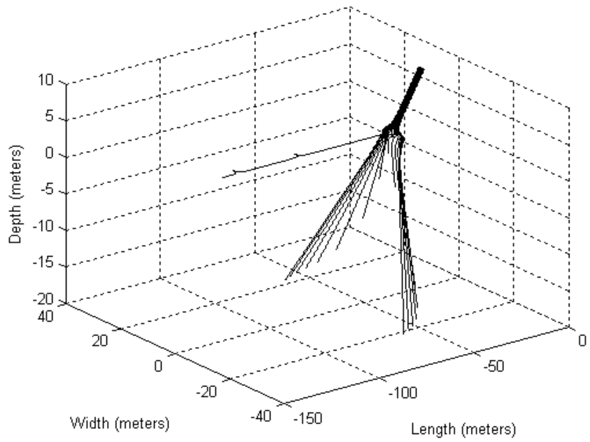

Figure 6: Results of initial efforts to modify the numerical code to account for k_2 to change with respect to time. The same general flow pattern is shown, but with fewer waves being absorbed by the vortex. Also, the center ray now has slight, but unexpected, periodic variations as it is carried along with the vortex.

Still further unsettling, the initial efforts to modify the code yield a solution more inaccurate. Figure 6 shows that the center mostly follows the straight line shown in Figure 3, but with slight periodic variation. Also, the rays traced are significantly spread out, refracted away from the dipole instead of being absorbed by it. It is impossible to tell at this stage if the rays that should pass through are doing so correctly. Though there may be more to modify with the code of the internal waves, it is also believed that the code for the dipole will need modification. Due to time constraints, these errors have yet to be cleared. However, it is known how to proceed to determine the exact cause for these errors. The equations are again being verified in the code. Likely the problem comes down to simple debugging of the subroutines involved in the numerical solution. It is expected that these problems will shortly be solved.

Additionally, the code for the counter-propagating scenario is not yet yielding any anticipated results and is clearly not yet functioning properly. This will require more time, though it is expected that the majority of problems associated with this case will be sorted out with the corrections of the errors in the co-propagating scenario.

Once the code is debugged and accurately finding the solution to the wave-vortex interaction, the results will have a variety of practical impact. Internal waves have large scale effects, are a significant source of atmospheric and oceanic mixing, and are a potential source of renewable energy. Through experimentation and observation, we know the breaking of internal waves drives global circulation patterns, yet we do not understand sufficiently how, where and when breaking and turbulence occur in the open ocean and atmosphere. Also, due to resolution capabilities of experimentation and observation, studies regarding geophysical flows are restricted to large scale analysis. However, much of what occurs on a global scale is a cumulative effect of many small-scale internal wave interactions, including three-dimensional processes. Additionally, the small-scale processes related to internal waves frequently obligate three-dimensional considerations.

As for the importance of the study particular to this paper, internal wave-vortex interactions are merely a single type of interaction that occurs naturally in geophysical stratified flows, but they are not uncommon; rather, they are quite the opposite. Understanding the relationship between the two phenomena in this interaction cannot only aid in the advancement of climate modeling and renewable energy potential, but it may also help in determining efficient flight patterns and shuttle-launch timing and locations. Re-entry methods can be improved, as well as inland landing sites, particularly as topography plays a distinct role in the generation of internal waves.

References

Billant, P., Brancher, P. & Chomaz, J. (1999). Three-dimensional stability of a vortex pair. *Physics of Fluids*, *11*, 2069-2077.

Broutman, D. & Young, W.R. (1986). On the interaction of small-scale oceanic internal waves with near-inertial waves. *Journal of Fluid Mechanics*, *166*, 341-358.

Godoy-Diana, R., Chomaz, J. & Donnadieu, C. (2006). Internal gravity waves in a dipolar wind: A wave-vortex interaction experiment in a stratified fluid. *Journal of Fluid Mechanics*, *548*, 281-308.

Javam, A., Imberger, J. & Armfield, S.W. (2000). Numerical study of internal wave-wave interactions in a stratified fluid. *Journal of Fluid Mechanics*, *415*, 65-87.

Moulin, F.Y. & Flór, J.-B. (2006). Vortex-wave interaction in a rotating stratified fluid: WKB simulations. *Journal of Fluid Mechanics*, *563*, 199-222.

Winters, Kraig B. & D'Asaro, Eric A. (1989). Two-Dimensional Instability of Finite Amplitude Internal Gravity Wave Packets Near a Crtical Level. *Journal of Geophysical Research*, *94*, 12,709-12,719.

Winters, Kraig B. & D'Asaro, Eric A. (1994). Three-dimensional wave instability near a critical level. *Journal of Fluid Mechanics*, *272*, 255-284.